LIFETIME AND DETECTABILITY OF BURIED ICE EXPOSED BY IMPACT CRATERING IN THE MOON'S PERMANENTLY SHADOWED REGIONS.

P. O. Hayne[1], [1]Laboratory for Atmospheric and Space Physics, University of Colorado Boulder, Boulder, CO 80303 (Paul.Hayne@Colorado.edu)

Introduction: Remote sensing observations have provided direct evidence of water ice on the surfaces of the Moon's permanently shadowed regions (PSRs) [1,2,3]. However, these detections indicate a heterogeneous distribution of volatiles, with some PSRs showing higher concentrations of ice in locations that are thermally equivalent to locations apparently lacking ice [4,5]. These observations are inconsistent with models of exospheric transport and cold-trap sequestration, which predict an essentially even distribution of surface frost over all cold traps with maximum temperatures < 110 K [6,7]. Here, we explore the hypothesis that destruction of H_2O frost at the surfaces of the PSRs is rapid compared to the supply rates [8] and that instead of gradual accumulation at the surface, the observed water ice signatures are due to ice exposed by discrete meteorite impacts.

Background: Although H_2O ice has been detected in the polar regions of the Moon [3,9], its distribution appears patchy and discontinuous over large PSRs where ice should be thermally stable on Gyr timescales [5]. Furthermore, the depth distribution and concentration of ice is uncertain. Evidence for buried ice is indirect, yet compelling: 1) the LCROSS impact excavated material from 2-3 m depth with higher concentrations of H_2O ice than the average surface abundance for all PSRs [9], and 2) an observed decrease in average depth/diameter ratios of craters toward the south pole is consistent with infill by 10's of meters of ice [10], covered by a (mostly) desiccated regolith layer comprising the uppermost ~1 m [11].

Approach and Methods: We model the rate of impacts and their resulting crater geometries using standard production functions and scaling laws [12,13]. The total area of cold traps for surface ice (based on the T_{max} < 110 K threshold) is $A_C \sim 10^4$ km² [14]. Although the area of subsurface ice stability is much larger, we do not consider this, because any impact-excavated ice exposed in sunlit regions will be vaporized rapidly. Our model includes a dry regolith layer with variable thickness, overlying an ice-rich layer with variable H_2O concentration. Once on the surface, the icy material is subjected to thermal and space-weathering processes; we investigate sublimation, UV photolysis, solar wind sputtering, and impact vaporization [15]. Inside the cold traps, non-thermal processes dominate [8].

Using the modeled impact rates, we can predict the area of icy regolith in the crater ejecta excavated over a given time interval. This interval Δt is taken as the time to remove a layer of H_2O resulting in an optically thick lag deposit (10 μm for near-IR wavelengths), typically corresponding to removal of ~1 μm of ice for pore-filling ice at ~50% porosity. We note that detection by ultraviolet spectroscopy [1] is limited to an even thinner (~1 μm) layer, and hence shorter ice lifetimes.

The surface area initially covered by the icy material is modeled based on the distance from the crater rim where the ejecta deposit reaches a critical thickness $z_{min} \sim d/2$, where d is the optical effective diameter of the ejecta particles (typically close to the mode diameter of ~100 μm. Ejecta thickness is modeled as $z(r) = z_0 r^{-B}$, where r is the distance from the crater rim, and $B \approx 3$. With a formation rate of impact craters with diameters from D to $D + \delta D$ equal to $N(D)$ (number per unit area per unit time), the area of icy ejecta on the surface exposed by these craters is $A_{ice}(D) = A_C N(D) \pi r_c^2 \Delta t$, where $r_c = \left(\frac{z_0}{z_{min}}\right)^{1/B}$ is the ejecta extent.

Anticipated Results: We calculate the expected area of exposed ice $A_{ice}(D)$ for different buried ice layer depths and destruction timescales Δt (Fig. 1). The resulting areas (or fractional areas of the PSRs) can be compared to observations of H_2O ice abundance (e.g., [3]). In this presentation, we will report our findings, and make testable predictions for future missions in order to better constrain the possible subsurface ice abundance in the lunar PSRs.

References: [1] Hayne P. O., et al. (2015), *Icarus*, *255*, 58-69. [2] Fisher, E. A. et al. (2017), *Icarus*, *292*, 74-85. [3] Li, S. et al. (2018), *PNAS*, *115*, 36. [4] Paige, D. A. et al. (2010), *Science*, 330, 479-482. [5] Landis, M. E., et al. (2022), *PSJ*, *3*, 39. [6] Watson, K., et al. (1961), *JGR*, *66*, 3033-3045. [7] Wilcoski, A. X., et al. (2022), *PSJ*, *3*, 99. [8] Farrell, W. M. et al. (2019), *GRL*, *46*, 8680-8688. [9] Colaprete, *A*. et al. (2010), *Science*, *330*, 463-468. [10] Rubanenko, L. et al. (2019), *Nature Geosci.*, *12*, 597-601. [11] Feldman, W. C. et al. (2001), *JGR*, *106*, 23231-23251. [12] Williams, J-P. et al. (2018), *JGR*, *9*, 2380-2392. [13] Collins, G. S. et al. (2005), *MAPS*, *40*, 817-840. [14] Hayne, P. O. et al. (2021), *Nature Astron.*, *5*, 169-175.

$t_{\mathrm{lifetime}} = 100$ kyr $t_{\mathrm{lifetime}} = 1$ Myr   Thermal Loss Only
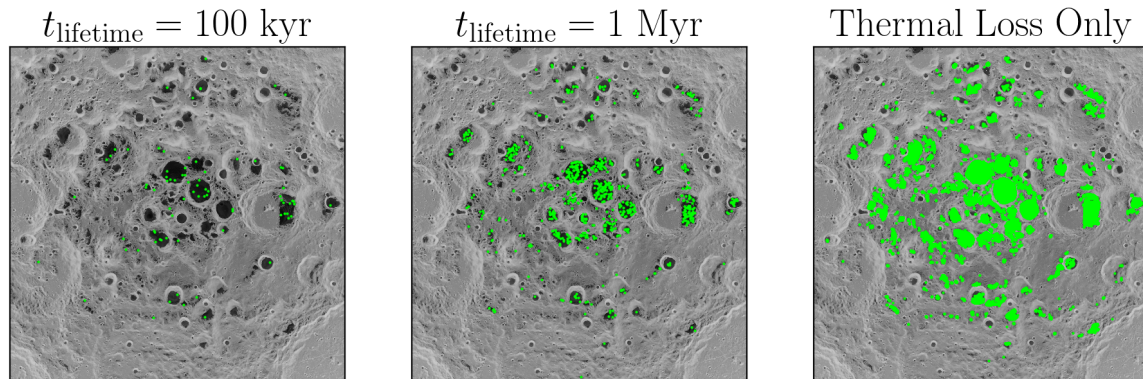
Figure 1: Simulated detections (green dots) of ice exposed by impact crater ejecta for different values of the ice lifetime on the surface, t_{lifetime}. In all cases, the lifetime is limited by thermal loss based on sublimation rates determined by the annual maximum temperature at each location (grayscale value in the background map). The values of t_{lifetime} are the upper limit assumed for non-thermal losses (e.g., micrometeorite vaporization, solar wind sputtering) [8]. We note a good correspondence to Moon Mineralogy Mapper detections [3] for $t_{\mathrm{lifetime}} \sim 0.1 - 1$ Myr, and also that the model with thermal loss only is inconsistent with those data.